

Title: Single-Catheter Dual-Modality Intravascular Imaging Combining IVUS and OFDI: A Holistic Structural Visualization of Coronary Arteries.

Authors: Jian Ren, PhD; Milen Shishkov, PhD; Martin L. Villiger, PhD; Kenichiro Otsuka, M.D, PhD; Seemantini K. Nadkarni, PhD; Brett E. Bouma, PhD

DOI: 10.4244/EIJ-D-20-00990

Citation: Ren J, Shishkov M, Villiger ML, Otsuka K, Nadkarni SK, Bouma BE. Single-Catheter Dual-Modality Intravascular Imaging Combining IVUS and OFDI: A Holistic Structural Visualization of Coronary Arteries. *EuroIntervention* 2021; Jaa-916 2021, doi: 10.4244/EIJ-D-20-00990

Manuscript submission date: 11 August 2020

Revisions received: 31 March 2021, 13 May 2021

Accepted date: 28 June 2021

Online publication date: 06 July 2021

Disclaimer: This is a PDF file of a "Just accepted article". This PDF has been published online early without copy editing/typesetting as a service to the Journal's readership (having early access to this data). Copy editing/typesetting will commence shortly. Unforeseen errors may arise during the proofing process and as such Europa Digital & Publishing exercise their legal rights concerning these potential circumstances.

Single-catheter dual-modality intravascular imaging combining IVUS and OFDI: A holistic structural visualization of coronary arteries

Author: Jian Ren¹, PhD; Milen Shishkov¹, PhD; Martin L. Villiger¹, PhD; Kenichiro Otsuka¹, MD, PhD; Seemantini K. Nadkarni¹, PhD; and Brett E. Bouma^{1,2}, PhD

Running title: Intravascular holistic structural visualization

Affiliation: ¹Wellman Center for Photomedicine, Massachusetts General Hospital, Harvard Medical School, Boston, MA USA; ²Institute for Medical Engineering and Science, Massachusetts Institute of Technology, Cambridge, MA USA.

Address for correspondence:

Jian Ren, PhD
Wellman Center for Photomedicine
Massachusetts General Hospital
Harvard Medical School
40 Blossom St
Boston, MA 02114, USA
jren@mgh.harvard.edu
Tel: +1 617-726-4350
Fax: +1 617-726-4103



Classifications: intravascular ultrasound, optical coherence tomography, innovation, pre-clinical research

Abbreviations:

CSA	cross sectional area
EEL	external elastic lamina
IV-HSV	intravascular holistic structural visualization
IVUS	intravascular ultrasound
LAD	left anterior descending artery
LCX	left circumflex artery
OCT	optical coherence tomography
OFDI	optical frequency domain imaging
PCI	percutaneous coronary intervention
TCFA	thin-capped fibroatheroma

Introduction

The large imaging depth of intravascular ultrasound (IVUS) combined with the high spatial resolution of optical coherence tomography (OCT) / optical frequency domain imaging (OFDI) offers refined insight into coronary atherosclerosis [1,2]. The integration of IVUS and OCT/OFDI into a single hybrid imaging catheter has previously been demonstrated *in vivo* in animals [3] and in patients [4]. Here, we present an improved IVUS-OFDI system that removes critical barriers to the clinical adoption of dual-modality imaging. Our catheter connects to the console through a fast interchange interface for simple and reliable operation. A novel algorithm fuses the IVUS and OFDI signals into a single combined image for Intravascular Holistic Structural Visualization (IV-HSV). We report on imaging experiments with human cadaver heart and swine *in vivo*, demonstrating the unique benefits of this system.

Methods

Our imaging console operates concurrent 1300 nm OFDI and 40 MHz IVUS imaging at 24.8 fps with a pullback speed of up to 20 mm/s. Displayed in the Central Illustration, the clinical grade imaging catheters have a 2.6 Fr / 3.2 Fr, 132 cm-long monorail design, compatible with standard 0.014" guidewires. The 1.3 mm-long rigid tip of the imaging probes comprises a side-viewing optical ball lens with a diameter of 200 μ m and a 0.5 mm-wide ultrasonic transducer, placed 300 μ m distally from the ball lens. The acoustic and optical beams are co-planar with respect to the catheter axis and feature an angle of 6° in the longitudinal direction, intersecting 2.8 mm from the sheath surface. A dual-channel rotary joint provides parallel optical and electrical connections and

enables a mechanical locking mechanism to secure the dual-channel connection with a simple click-on, allowing for fast interchange of the disposable catheters.

To aid the interpretation of IVUS and OFDI, the co-registered images were accurately scaled to common spatial coordinates and computationally fused into a single structural map - IV-HSV - based on image content. Starting from the lumen, the algorithm seamlessly transitions from the OFDI signal to the IVUS signal at an optimal depth, automatically computed for each radial profile using an OFDI intensity threshold. This results in near-lumen structures being visualized with the high definition of OFDI, ideally complemented with the IVUS image of deeper lying features, overall preserving the most clinically relevant information.

Through the National Disease Research Interchange, a cadaver human heart was collected within 24 hours after death and stored at -80 degree Celsius. Tissues were thawed before imaging experiments. Multiple coronary artery segments, including perivascular tissue, were resected from the heart. A custom fixture was used to mount the artery segments and ensure accurate co-registration with histopathology [5]. During pullback imaging, saline was manually flushed through the segments. After imaging, frozen sections of the arterial samples were processed for hematoxylin-eosin (H&E) and trichrome staining.

To test the system in a clinical setting, we conducted intravascular imaging *in vivo* in a healthy Yorkshire pig. A 7 Fr guide catheter was placed through the carotid artery to gain access to the coronary arteries. Both the left anterior descending artery (LAD) and left circumflex artery (LCX) were catheterized using a 0.014" guidewire. A total of fourteen 60 mm-long pullbacks were acquired at various pullback speeds (5-

20 mm/s). Contrast injection was manually performed to displace circulating blood in the imaged coronary arteries.

Results

First, we performed dual-modality imaging of a human cadaver heart, to visualize various features of coronary atherosclerosis. Exemplary for fibroatheroma, the IV-HSV image in Figure 1(A1) renders the lumen and the shallow fibrous cap as captured by OFDI, complemented by the outer border of the thick cap and the entire vessel wall cross-section as disclosed by IVUS. Notably, the vessel injury at 6-8 o'clock is visualized in high resolution with OFDI in IV-HSV, as it would be difficult to identify in IVUS. Furthermore, the IV-HSV image enabled evaluation of the external elastic lamina (EEL) cross sectional area (CSA) owing to the IVUS signal. Although IVUS can also provide an estimation of luminal CSA, plaque burden estimation in IV-HSV is simplified by the clear lumen definition of OFDI. A fibro-calcified plaque is also included in Figure 1(B).

Next, we tested the use and performance of the dual-modality system in the catheterization laboratory by imaging in a healthy swine (Figure 2). Owing to the intrinsic co-registration, OFDI and IVUS images show matching side branch locations. Luminal CSA measured independently with OFDI and IVUS reveal excellent Pearson's correlation ($r = 0.97$, $p < 0.001$, $N = 40$) (Figure 2(B)). The Bland-Altman plot (Figure 2(C)) suggests neither the measurement bias (-0.07 mm^2) nor the limits of agreement (0.25 and -0.38 mm^2) are clinically important. The averaged Hausdorff distance and mean distance between the lumen borders segmented in both modalities are $160 \text{ }\mu\text{m}$

and 56 μm with standard deviations of 48 μm and 22 μm , respectively [6]. This analysis suggests intrinsic co-registration of the two modalities, owing to the accurate alignment of the optical and ultrasound beams.

Discussion

To date, dual-modality systems presented OCT and IVUS images either as separate panels, making spatial correlation across modalities difficult, or as color-encoded overlay, which complicates thorough inspection as the layers shade each other. The large difference in resolution and speckle size between OCT and IVUS further aggravate this shading effect. In contrast, IV-HSV offers a single-color, easy-to-comprehend view, enabling effortless interpretation of critical artery features that are relevant for guiding percutaneous coronary intervention (PCI).

As demonstrated by our results, this hybrid imaging system offers unique insights into vessel pathology. A first example is the simultaneous visualization of both near-lumen microstructures and deep lesion morphology in a single map. In the IV-HSV of Central Illustration, a vessel injury at 7 o'clock was clearly imaged by OFDI and a deep calcification was disclosed by IVUS at 9 o'clock. A second example is the improved characterization of calcification by the co-registered dual-modality imaging. While IVUS identifies deep calcification that OFDI alone is unable to detect (Central Illustration), OFDI can assess the thickness of shallow calcification (Figure 1(B)), in addition to its length and arc angle. Calcium scoring including thickness parameters has been shown to reliably predict stent expansion [7]. Another possible benefit of IV-HSV is a potentially more accurate estimation of plaque burden than with either IVUS or OCT/OFDI alone,

because it combines the robust mapping of the EEL owing to the deep penetration of IVUS with the accurate delineation of the lumen owing to the improved resolution of OCT/OFDI. This may refine plaque burden as a robust predictor of PCI outcomes [8].

Limitations

Imaging of coronary atherosclerosis was performed in a single cadaver heart and a healthy swine was used for *in vivo* imaging. Clinical studies will be needed to demonstrate the diagnostic value of dual-modality imaging in a clinical setting. The fusion algorithm relies on OFDI signal to define the transition from OFDI to IVUS, which could result in non-optimal partitioning of the two modalities due to artifacts in OFDI images. Finally, dual-modality imaging requires blood clearing through the injection of contrast media or saline for OFDI imaging.

Conclusions

This study demonstrates the technical capability of our dual-modality system and suggests its potential for aiding PCI. Acquired concurrently with a single pullback of a hybrid imaging catheter, intrinsically co-registered IVUS and OFDI images provide complementary diagnostic information. IV-HSV fuses them into a single-color, easy-to-comprehend map, that provides interventionists with a holistic and accurate overview of the coronary arterial wall and its disease burden.

Acknowledgements: K.O. acknowledges partial support from the Japan Heart Foundation / Bayer Yakuhin Research Grant Abroad, the Uehara Memorial Foundation Postdoctoral Fellowship, and the Japan Society for the Promotion of Science Overseas Research Fellowship. The authors acknowledge Leon Ptaszek MD, PhD and Moussa Mansour, MD at the Department of Cardiology, Massachusetts General Hospital for *in vivo* swine imaging; Diane Tshikudi, MS and Pallavi Doradla, PhD at the Wellman Center for Photomedicine, Massachusetts General Hospital for their assistance in cadaver tissue preparation and histology.

Copyright EuroIntervention

Funding: This work was supported by the National Institutes of Health (P41EB015903, K99AG059946, and R01HL119065) and by Terumo Corporation.

Conflict of Interest: Massachusetts General Hospital has patent licensing arrangements with Terumo Corporation. B.E.B. and M.L.V. have the right to receive royalties as part of the licensing arrangements. All other authors have reported that they have no relationships relevant to the contents of this paper to disclose.

Copyright EuroIntervention

Reference:

1. Fujii K, Hao H, Shibuya M, Imanaka T, Fukunaga M, Miki K, Tamaru H, Sawada H, Naito Y, Ohyanagi M, Hirota S, Masuyama T. Accuracy of OCT, Grayscale IVUS, and Their Combination for the Diagnosis of Coronary TCFA. *JACC Cardiovasc Imaging*. 2015;8:451 LP – 460.
2. Nakano M, Yahagi K, Yamamoto H, Taniwaki M, Otsuka F, Ladich ER, Joner M, Virmani R. Additive Value of Integrated Backscatter IVUS for Detection of Vulnerable Plaque by Optical Frequency Domain Imaging: An Ex Vivo Autopsy Study of Human Coronary Arteries. *JACC Cardiovasc Imaging*. 2016.
3. Li J, Li X, Mohar D, Raney A, Jing J, Zhang J, Johnston A, Liang S, Ma T, Shung KK, Mahon S, Brenner M, Narula J, Zhou Q, Patel PM, Chen Z. Integrated IVUS-OCT for Real-Time Imaging of Coronary Atherosclerosis. *JACC Cardiovasc Imaging*. 2014;7:101–3.
4. Sheth TN, Pinilla-Echeverri N, Mehta SR, Courtney BK. First-in-Human Images of Coronary Atherosclerosis and Coronary Stents Using a Novel Hybrid Intravascular Ultrasound and Optical Coherence Tomographic Catheter. *JACC Cardiovasc Interv*. 2018;11:2427–30.
5. Gardner CM, Tan H, Hull EL, Lisauskas JB, Sum ST, Meese TM, Jiang C, Madden SP, Caplan JD, Burke AP, Virmani R, Goldstein J, Muller JE. Detection of Lipid Core Coronary Plaques in Autopsy Specimens With a Novel Catheter-Based Near-Infrared Spectroscopy System. *JACC Cardiovasc Imaging*. 2008;1:638–48.
6. Huttenlocher DP, Klanderma GA, Rucklidge WJ. Comparing images using the

- Hausdorff distance. *IEEE Trans Pattern Anal Mach Intell.* 1993;15:850–63.
7. Fujino A, Mintz GS, Matsumura M, Lee T, Kim S-Y, Hoshino M, Usui E, Yonetsu T, Haag ES, Shlofmitz RA. A new optical coherence tomography-based calcium scoring system to predict stent underexpansion. *EuroIntervention J Eur Collab with Work Gr Interv Cardiol Eur Soc Cardiol.* 2018;13:e2182–9.
 8. Schuurman AS, Vroegindewey MM, Kardys I, Oemrawsingh RM, Garcia-Garcia HM, van Geuns RJ, Regar E, Van Mieghem NM, Ligthart J, Serruys PW, Boersma E, Akkerhuis KM. Prognostic Value of Intravascular Ultrasound in Patients With Coronary Artery Disease. *J Am Coll Cardiol.* 2018.

Figure Legends:

Central Illustration

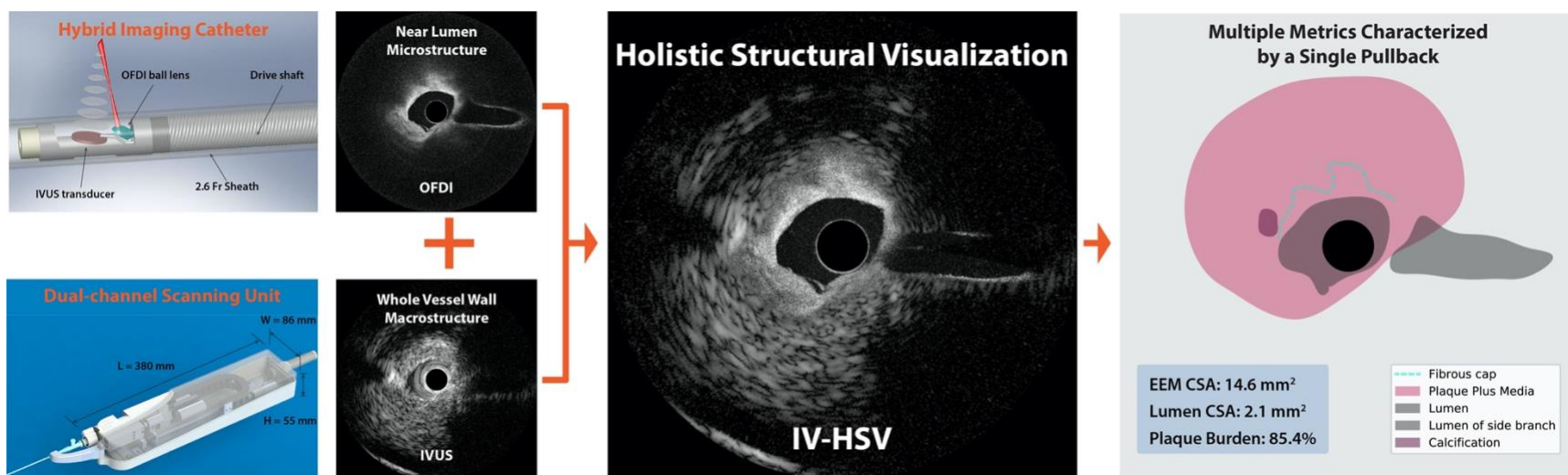
Hardware and software work together to provide one complete map of vessel wall structures that can improve the diagnosis of coronary plaques during cardiac catheterization procedures. (The pullback speed was 10 mm/s.)

Figure 1. Representative holistic structural visualization (IV-HSV) of human cadaver coronary artery.

Representative images of a fibroatheroma (**A1 to A6**) and a fibro-calcified plaque (**B1 to B6**). IV-HSV images (**A1 and B1**), combining the OFDI image (**A2 and B2**) and IVUS image (**A3 and B3**). (**A4**) Segmentation of various plaque features in the IV-HSV image (**A1**), and isolated visualization of the segmented structures, enabling computation of plaque burden (**A5**). (**A6**) Matching trichrome-stained histopathology. A dissection of the coronary artery appears from 6 to 8 o'clock. The IV-HSV image (**A1**) visualizes relevant details of the dissected vessel wall by optimally merging the IVUS and OFDI appearances. The yellow stars in (**A4**) indicate necrotic cores, confirmed by histopathology (yellow stars in (**A6**)). (**B4 and B5**) show the magnified views of the square areas of interest indicated in (**B1**). (**B6**) Matching histopathology, stained with hematoxylin and eosin. Scale bars in (**A2, B2**) apply to both (**A2, B2**) and (**A3, B3**), respectively. The pullback speed was 10 mm/s.

Figure 2. *In vivo* swine catheterization and intravascular imaging.

(A) Coronary angiogram showing the left coronary arteries during pullback imaging. **(B)** Pearson's correlation analysis of 40 luminal CSAs measured independently with OFDI and IVUS across a 32-mm-long segment of the LAD with a large variation of lumen size and shape, acquired at 10 mm/s pullback speed. **(C)** Bland-Altman plot of the 40 luminal CSAs measured independently with OFDI and IVUS. **(E, F, and D)** are intrinsically co-registered OFDI, IVUS, and cross-sectional IV-HSV images acquired in the LAD. The yellow stars indicate the locations of side branches. The 'sew up' artifact at 9 o'clock is a result of the helical scan pattern of 'rotation-pullback' imaging and heart motion during the intervention. Both **(B)** and **(C)** show excellent agreement between measurements with the two modalities, accounting to the accuracy of the intrinsic co-registration of the dual-modality imaging system. The green lines in **(E and F)** are the lumen segmentations. **(D-F)** share the same scale bar in **(D)**.



Disclaimer : As a public service to our readership, this article -peer reviewed by the Editors of EuroIntervention and external reviewers - has been published immediately upon acceptance as it was received in the last round of revision. The content of this article is the responsibility of the authors.

